Predicted roles of defects on band offsets and energetics at CIGS (Cu(In,Ga)Se2/CdS) solar cell interfaces and implications for improving performance

Hai Xiao and William A. Goddard III

Citation: The Journal of Chemical Physics **141**, 094701 (2014); doi: 10.1063/1.4893985
View online: http://dx.doi.org/10.1063/1.4893985
View Table of Contents: http://scitation.aip.org/content/aip/journal/jcp/141/9?ver=pdfcov
Published by the AIP Publishing

Predicted roles of defects on band offsets and energetics at CIGS ($Cu(In,Ga)Se_2$/CdS) solar cell interfaces and implications for improving performance

Hai Xiao (肖海) and William A. Goddard III[a)]
Materials and Process Simulation Center, California Institute of Technology, Pasadena, California 91125, USA

(Received 30 June 2014; accepted 14 August 2014; published online 2 September 2014)

The laboratory performance of CIGS ($Cu(In,Ga)Se_2$) based solar cells (20.8% efficiency) makes them promising candidate photovoltaic devices. However, there remains little understanding of how defects at the CIGS/CdS interface affect the band offsets and interfacial energies, and hence the performance of manufactured devices. To determine these relationships, we use density functional theory with the B3PW91 hybrid functional that we validate to provide very accurate descriptions of the band gaps and band offsets. This confirms the weak dependence of band offsets on surface orientation observed experimentally. We predict that the conduction band offset (CBO) of perfect $CuInSe_2$/CdS interface is large, 0.79 eV, which would dramatically degrade performance. Moreover we show that band gap widening induced by Ga adjusts only the valence band offset, and we find that Cd impurities do not significantly affect the CBO. Thus we show that Cu vacancies at the interface play the key role in enabling the tunability of CBO. We predict that Na further improves the CBO through electrostatically elevating the valence levels to decrease the CBO, explaining the observed essential role of Na for high performance. Moreover we find that K leads to a dramatic decrease in the CBO to 0.05 eV, much better than Na. We suggest that the efficiency of CIGS devices might be improved substantially by tuning the ratio of Na to K, with the improved phase stability of Na balancing phase instability from K. All these defects reduce interfacial stability slightly, but not significantly. © *2014 AIP Publishing LLC*. [http://dx.doi.org/10.1063/1.4893985]

I. INTRODUCTION

Harvesting solar energy, through direct transformation into electrical power by photovoltaic devices, is a most promising approach to renewable energy alternatives, and indeed the global operating capacity for solar photovoltaics is increasing steadily.[1] Currently, crystalline silicon technology dominates industrial solar cell production,[2] but thin film technology for solar cells would provide flexibility in both production and implementation.[3] Among all thin film absorber materials, $Cu(In,Ga)Se_2$ (CIGS) has reached the highest conversion efficiency exceeding 20% on rigid substrates in laboratory-scale,[4] with efficiency on flexible substrates increasing rapidly,[5,6] but that the efficiency of manufactured modules and panels lags behind considerably, raising the quest for identifying key factors in quality control of composition and structure. A significant characteristic of CIGS absorbers is the universal presence of such structural defects as Cu vacancies and Na impurities, which correlate strongly with device performance. We expect that understanding these correlations would help improve CIGS solar cell manufacturing processes to achieve high performance and might point the way toward designing novel absorber materials.

Experimentally, it is well established that Cu deficiencies near the CIGS/CdS interface is an essential characteristic of highest efficiency CIGS solar cells.[7–9] It has been suggested that this may be because of reduced recombination,[10] but others consider that is not likely the major responsible for the effect of Cu vacancies on performance.[11]

Additionally, incorporation of Na,[9,10,12] is widely accepted as a key ingredient in building the best performance devices, but the origin of this effect remains debated, with suggestions that it may affect film growth (grain sizes and crystal orientation)[13–17] and p-type conductivity.[16,18,19] None of these speculations has yet been confirmed as crucial for the boost in performance. Indeed K has recently been proposed[6] to provide a beneficial alternative. In addition, it is generally observed that Cd dopants are introduced by diffusion into CIGS absorbers close to the interface with CdS buffer layers,[20–22] resulting in the formation of a buried homojunction,[23] but this is suggested to have limited influence on cell efficiency.[24]

Despite numerous experimental studies, an atomistic understanding of the roles of such defects on device performance is hindered by difficulties in decoupling and probing directly the effects from various factors. Consequently, we carried out quantum mechanics (QM) studies to provide an understanding of these phenomena.

Density functional theory (DFT)[25,26] methods of QM are widely used to investigate the relationship between chemistry and functionality of materials, and some DFT efforts have previously been applied toward such aspects of CIGS solar cells, as defect formation[19,27–32] and levels.[33–35]

The most important aspect of CIGS solar cells is the CIGS/CdS interface, where the essential physics of

a)Author to whom correspondence should be addressed. Electronic mail: wag@wag.caltech.edu.

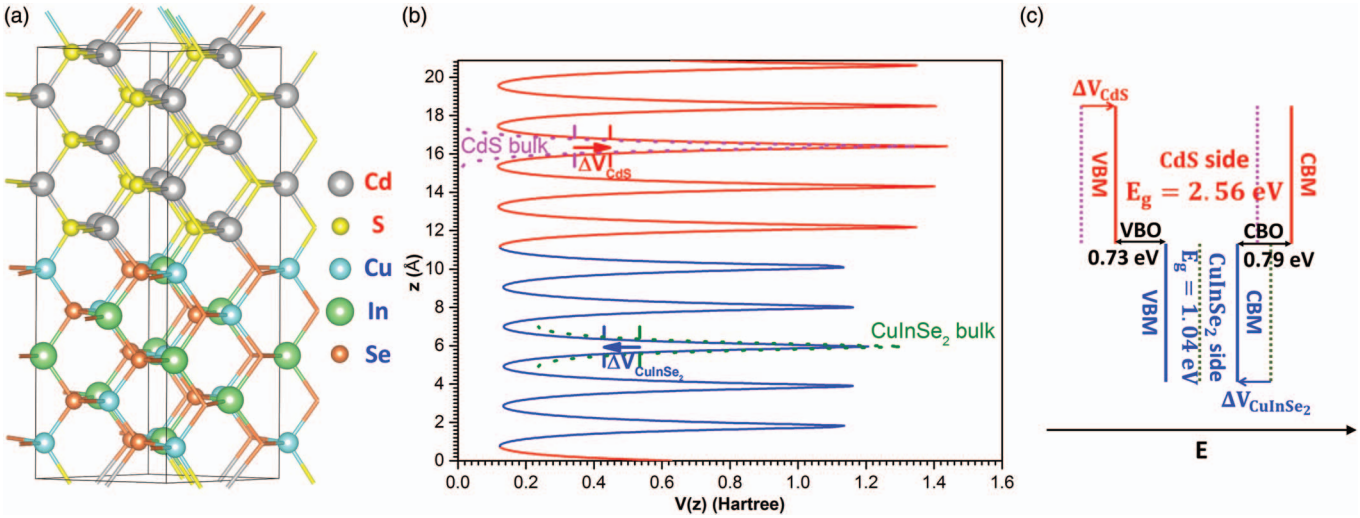

FIG. 1. Illustration of the computation of band offsets for the $CuInSe_2$/CdS (110) interface (a) supercell structure with 5 layers for each material where the vertical axis is the [001] or z axis, (b) electrostatic potential averaged over the xy plane plotted along the z direction. At the middle layer of each side, we compare to results from bulk calculations (dotted lines). This is used to obtain the potential shift ΔV for each material and (c) the final band alignment. Note that all potential shifts are exaggerated for clarity.

photovoltaics takes place. It is here that the defects mentioned above have their highest concentrations and their greatest impact. Therefore, the aim of our studies is to provide a theoretical basis for understanding of roles of defects in the CIGS/CdS interface.

In this paper, we first establish the accuracy of the B3PW91 flavor of DFT methodology for predicting band offsets through benchmarks studies on (110) and (112) $CuInSe_2$/CdS interfaces. Then we determine the effects of Cu vacancies, and doping with Ga, Na, K, and Cd on both band offsets and interfacial energies. To do this we constructed interfaces between CdS and CIGS with various defects. These results are used to recommend changes to optimize solar cell performance.

II. COMPUTATIONAL DETAILS

It is generally understood that the LDA or GGA (PW91 or PBE) flavors of DFT lead to band gaps that are 1–2 eV too small.[36,37] For these methods it is popular to add in a Hubbard self-interaction correction (U) to improve the band gap[38] or to include perturbative many-body approximation (G_0W_0).[39] Our approach is instead to use hybrid DFT functionals[40] that we have shown to provide accurate band gaps for semiconductors and insulators.[41–45] In particular we showed that the hybrid functional B3PW91,[40] gives accurate band gaps (within 0.1 eV) for the semiconductors considered in this study.[45]

All calculations were performed with the CRYSTAL09 package[46] which uses local atomic Gaussian-type basis sets rather than plane waves. This enables fast evaluation of the Hartree-Fock exchange terms required for hybrid DFT method (the evaluation of exact exchange for plane wave basis sets is very expensive).

We used all-electron basis sets of triple-ζ quality for Na, S, and K,[47,48] but for Cu, Ga, Se, Cd, and In, we used the SBKJC Relativistic effective core potentials (based on angular momentum projection operators[49,50]) and the associated basis sets.[51] Thus we treat explicitly just the outer 19 electrons for Cu, 21 for Ga, 6 for Se, 20 for Cd, and 21 for In. We optimized the valence and polarization Gaussian exponents of all basis sets for ideal crystal structures (details are given in the supplementary material[52]) to reduce linear dependency. Note that we neglected spin-orbit coupling (SOC), because all the systems considered here are closed-shell, and the lowest conduction bands are dominant by *s*-type atomic orbitals, there is only second-order SOC, which is small. For example, the contribution of SOC to band gaps in CdS and InP are calculated to be only 0.03 and 0.08 eV.[53]

An extra-large grid, consisting of 75 radial points and 974 angular points, was used for accurate integration, and the reciprocal space was sampled by Γ-centered Monkhorst-Pack scheme[54] with a fine resolution of around $2\pi \times 1/40$ Å^{-1}.

We employed the Average Electrostatic Potential (AEP) method,[55] rather than the core level method as discussed later, to provide reference levels necessary for connecting the macroscopic band energy levels for the bulk systems and the interfaces.[56] The electrostatic potential was evaluated at each point by the range separation and multipolar expansion scheme[57,58] implemented in CRYSTAL09, setting ITOL = 15 and IDIPO = 6 for accuracy. In order to converge the integrals of electrostatic potentials to within 0.01 eV, we adopted grids with resolution of 0.01 Å.

Figure 1 illustrates the procedure of aligning band energies of our interface calculations with those of the bulk system.

- First, we constructed the interface based on the bulk structures.
- Then we optimized fully both the atomic positions and the supercell lattice parameters, while applying symmetry constraints to maintain a perfect matching at the interface (all coordinates and

symmetry constraints are provided in the supplementary material[52]).

- Then we averaged the electrostatic potential within the xy plane as a function of the interface direction, z to obtain V(z). Here the middle layer of each material, uniquely defined between minima of V(z), was further averaged and compared to the V(z) from bulk calculations to deduce the shift in the reference levels.
- Finally, the valence band maximum (VBM) and conduction band minimum (CBM) in each bulk system were aligned to obtain the valence band offset (VBO) and the conduction band offset (CBO).

Note that, for theoretical consistency, all values, including band gaps and lattice parameters of bulks, are from calculations of the same B3PW91 level, with no use of experimental results.

In constructing interface models, lattice matching of two sides is an inevitable issue, but all cases throughout this study have lattice mismatch within 0.7%, which we found to give at most 0.06 eV error in relative electronic levels.

III. RESULTS AND DISCUSSION

A critical problem in modeling interfaces with three-dimensional periodic boundary conditions is the artificial interaction introduced between the interface and its image. However, if local charge neutrality holds at the interface, such dipole-dipole interactions decay as r^{-3}, so that it is of negligible influence for modest distances between the interfaces. Consequently we first performed benchmark calculations to find an optimal interface spacing that is large enough to exclude significant interface-interface interaction but reasonably small for affordable computation cost. Table I summarizes this validation, which shows clearly that convergence is achieved with ~10 Å distance between interfaces for the AEP method. This leads to convergence of interfacial energies within 0.004 J/m^2 and band offsets within 0.01 eV. Most importantly the predicted VBO = 0.73 eV agrees with the experimental results of VBO = 0.8 ± 0.1 eV.[59] This error of only 0.07 eV, is within the mean absolute error of 0.09 eV for predicting band gaps from B3PW91.[45] This demonstrates both stability and reliability of our methodology.

TABLE I. Convergence of interface thickness (d), interfacial energy (σ), VBO (ΔEv) and CBO (ΔE_c) with respect to number of layers of each side (L) and the interface-interface distance (D) for $CuInSe_2$/CdS interfaces parallel to (110) and (112). Here the interfacial energy is defined as $\sigma = \frac{E_{\text{interface}} - \sum_i E_{bulk\,i}}{A}$, where both $E_{\text{bulk,i}}$ are scaled proportionally to match numbers of units in the supercell and A is the interface area. The superscript CL indicates band offsets calculated with core level method.

	Nonpolar (110)				
L	3	5	7	9	Expt.[a]
D (Å)	6.27	10.47	14.68	18.89	
d (Å)	2.08	2.07	2.08	2.08	
σ (J/m^2)	0.051	0.048	0.052	0.052	
ΔE_v (eV)	0.67	0.73	0.72	0.72	0.8 ± 0.1
ΔE_c (eV)	0.85	0.79	0.80	0.80	
(ΔE_v)CL (eV)	1.00	1.11	1.13	1.10	
	Polar (112)				
L	3	6			
D (Å)	10.30	20.61			
d (Å)	2.56	2.56			
σ (J/m^2)	0.042	0.040			
ΔE_v (eV)	0.69	0.67			
ΔE_c (eV)	0.83	0.85			

[a]Reference 59.

A popular alternative to AEP is to determine band offsets by using core levels as a reference.[60] As shown in the supplementary material,[52] we find that use of the core levels from different elements leads to some fluctuations, with changes in the predicted CBO of up to 0.07 eV (as observed previously[60]). We found that the combination with the most stable convergence is: In (4s) for $CuInSe_2$ side and Cd (4s) for CdS side. (Due to the use of ECP, the deepest available core levels are S (1s), In (4s), Cu (3s), and Cd (4s), in ascending energy order.) The results are shown in Table I. At a large distance of ~19 Å between interfaces, an oscillation of 0.03 eV is still remains in the calculated VBO, leading to a result 0.3 eV larger than the experimental value. In principle, with semi-local exchange-correlation (XC) functionals, core levels and AEP have equivalent convergence and shift. However, the global hybrid functional B3PW91 used here includes non-local Hartree-Fork exchange, which makes XC potential orbital-dependent, so the Kohn-Sham orbitals and eigenvalues are more coupled and thus tricky to converge with respect to the interface-interface distance, i.e., they are sensitive to the presence of interface. In contrast, AEP is directly derived from electron density, which is subject to variational principle and thus steady convergence.

Table I includes results for both the (110) nonpolar interface and the polar (112) interface commonly observed in CIGS solar cells.[61] Although the polar nature of this orientation raises problems in surface calculations due to charge separation, local neutrality still holds in each layer of the perfect matching interface models as shown in Figure 2. Thus the argument for convergence mentioned above is valid here. Indeed, Table I shows convergence at about 10 Å in polar cases, similar to the nonpolar ones.

The calculated VBO value of 0.69 eV in (112) is only 0.04 eV smaller than for (110), indicating weak dependence of band offsets on surface orientation, which is consistent with experimental observation.[62] This indicates that the potential shift of each semiconductor side in the interface is insensitive to the detailed local structure or dipole of the interface, whether it is nonpolar or polar. Rather it is determined by the intrinsic nature of the atoms at both sides. Indeed the average electrostatic potential we use demonstrates such character, validating that it provides the proper theoretical reference linking microscopic interface modelling with macroscopic screening in semiconductor interfaces.

Strikingly, our calculations show that for the perfect interface the CBO = 0.83 eV, which is far from optimal, where 0–0.4 eV,[63] is thought to be best. Such a high CBO would provide a barrier preventing transport of photo-generated electrons from absorber to buffer layer. This result would appear

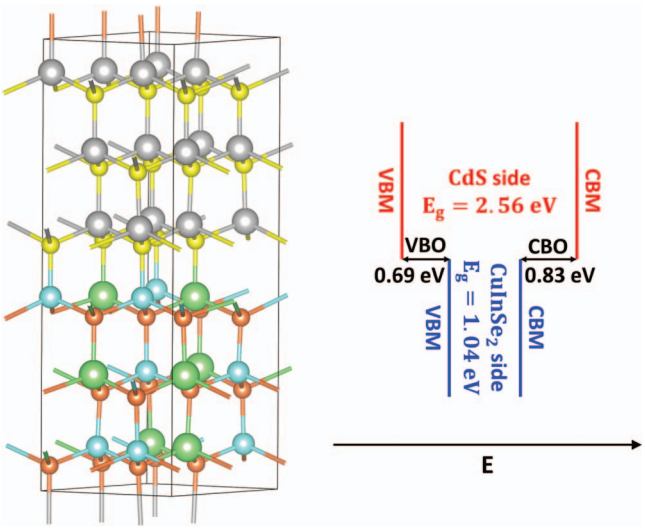

FIG. 2. The $CuInSe_2$/CdS (112) polar interface model and the calculated band alignment. This CBO and VBO are within 0.04 eV of the (110) case in Figure 1.

to contradict the excellent performance of CIGS/CdS based solar cells. Consequently we carried out investigations to resolve the inconsistency.

We expected that the CBO is strongly affected by the distribution of vacancies and defects, so we replaced with Ga one out of the four symmetric In atoms in the conventional cell of $CuInSe_2$, leading to $CuIn_{0.75}Ga_{0.25}Se_2$, which mimics the Ga concentration of ∼0.3 in the best performance solar cells and which has a lattice mismatch within 0.7% (one additional Ga substitution in our cell would give >1% mismatch, while the limiting case $CuGaSe_2$ has more than 5% lattice mismatch with CdS).

Figure 3(a) shows the supercell of the $CuIn_{0.75}Ga_{0.25}Se_2$/CdS(110) interface. We were surprised to find that the increase of 0.13 eV in the absorber band gap goes entirely to decreasing VBO to 0.56 eV, while the CBO stays at 0.83 eV. This implies that the valence region of this absorber is more sensitive to such changes in the chemical environment addressed by band gap engineering, indicating that the CBO is not easily tuned. Indeed we find that for Cu-rich CIGS, the top of the valence band is dominated by the Cu 3*d* orbitals (see the supplementary material[52]), suggesting that Cu vacancy could have a large effect.

Experimentally, the structure of the commonly observed Cu deficient phase $CuIn_3Se_5$ has been interpreted in terms of several quite different structural models,[28] with no consensus. However, some theoretical models have been proposed to investigate this phase.[27–29] Following previous work, we used a pristine $\sqrt{2} \times \sqrt{2} \times 1$ cell containing $Cu_8In_8Se_{16}$ to derive two Cu-poor structures having distinctly different Cu vacancy concentrations, i.e.,

- $Cu_5In_9Se_{16}$ with 2 Cu vacancies or 12.5 at% and one In at a Cu site,
- $CuIn_5Se_8$, with 2 Cu vacancies or 25 at% and one In at a Cu site.

For each case we examined all possible configurations and adopted the one with the lowest energy (details are given in the supplementary material[52]). We find that just as for Ga alloying, the Cu vacancies increase the band gap. Here the B3PW91 predicted band gap of 1.30 eV for $CuIn_5Se_8$ phase is in excellent agreement with the experimental value of 1.27 eV.[64]

Figure 3(b) shows the interface models of $Cu_5In_9Se_{16}$/CdS while Fig. 3(c) shows $CuIn_5Se_8$/CdS. For $Cu_5In_9Se_{16}$ we find that the 12.5% concentration of Cu vacancy increases the band gap by 0.03 eV but does not change the CBO at all. However, the $CuIn_5Se_8$ case with 25% depletion of Cu constituents increases the band gap by 0.26 eV while increasing the VBM due to the reduction in the number of chemical bonds. This tunes the CBO to 0.46 eV, very close to the optimal value. These results corroborate the speculation that Cu 3*d* electrons dominate the valence band maximum region, so that the VBO depends on the electronic structure engineering, while sufficient concentration of Cu vacancies enables tunability of the CBO. We suggest that this underlies the high efficiency of CIGS solar cells, which correlate with the presence of Cu deficient phases at the interface.

We also examined the interfacial energies, finding that Ga alloying slightly decreases the interface stability, increasing σ from 0.048 to 0.056 J/m^2 for the $CuIn_{0.75}Ga_{0.25}Se_2$/CdS case while Cu vacancies dramatically decrease interfacial

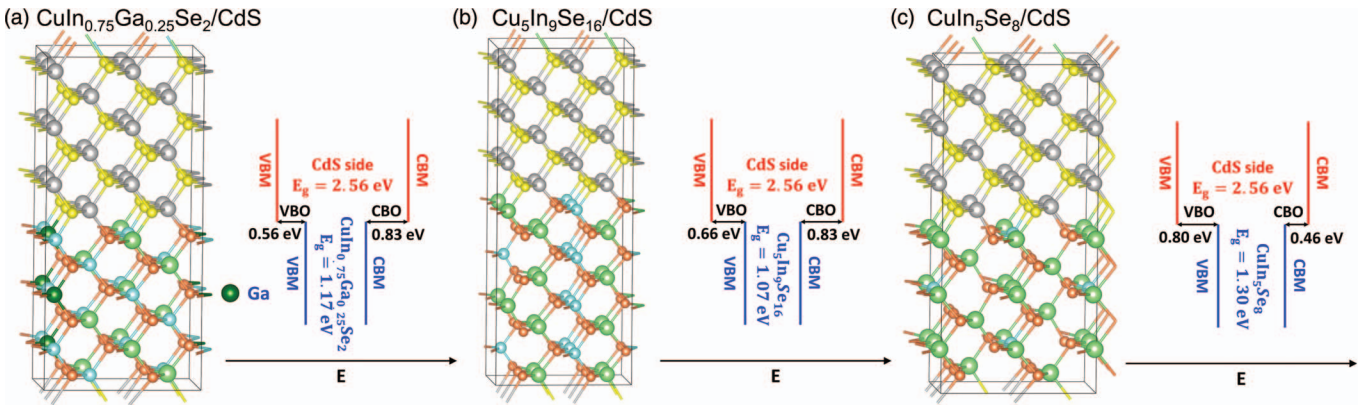

FIG. 3. The interface models and calculated band alignments of (a) $CuIn_{0.75}Ga_{0.25}Se_2$/CdS, where we see that the band gap increase of 0.10 eV goes entirely to decreasing the VBO, (b) $Cu_5In_9Se_{16}$/CdS and (c) $CuIn_5Se_8$/CdS, which increases the band gap by 0.26 eV while decreasing the CBO by 0.33 eV.

stability with $\sigma = 0.129$ J/m^2 for $Cu_5In_9Se_{16}$/CdS and 0.107 J/m^2 $CuIn_5Se_8$/CdS. This decrease in interfacial stability is the consequence of weaker bonding at the interface. Partly this results from stretching the Ga-S bonds from their preferred length of 2.32 (in $CuGaS_2$ bulk) to 2.36 Å at the interface and partly it is because of fewer chemical bonds due to Cu vacancies. However, these interfacial energies are all rather small, so that the interfacial stability effects are far less important than the band offsets.

Since a Cu deficient phase is universally present at the CIGS interface, the other dopants were modeled based on the $Cu_5In_9Se_{16}$ structure proposed above. Previous calculations showed the preferred sites to be substitutional Na_{Cu} and Cd_{Cu},[19,31] so we formed the bulk structures based on replacing two Cu atoms by two Na, two K, or one Cd. That is we considered $Na_2Cu_3In_9Se_{16}$, $K_2Cu_3In_9Se_{16}$, and $CdCu_3In_9Se_{16}$. Again we calculated all possible configurations and chose the ones with the lowest total energy (details are given in the supplementary material[52]). These configurations are consistent with each other and lead to a ratio of Cu:In:Se that is close to 1:3:5. We should point out that the optimal experimental atomic concentration of Na doping is ~0.1%, but that Na accumulates on surfaces up to ~1 at%.[65] Our model bulk $Na_2Cu_3In_9Se_{16}$, has 6.7 at% Na. Nevertheless we consider that this model is reasonable to probe the physics.

Figures 4(a) and 4(b) show the interfacial models of $Na_2Cu_3In_9Se_{16}$/CdS and $K_2Cu_3In_9Se_{16}$/CdS. Indeed, we find that Na tunes the CBO from 0.83 eV to 0.45 eV while K tunes it to 0.05 eV. Thus both alkalis move toward the optimal values while changing the overall band gap by 0.27 eV for Na and 0.20 eV for K. That a different mechanism is responsible, is clearest for the K case: where the reduction of CBO by 0.78–0.05 eV is mostly due to increasing the VBM by 0.58 eV. Thus the presence of these very positively charged alkali elements attract electrons in the valence region (from either Cu 3*d* or Se 4*p*) pushing up the energy. Therefore, it is the electrostatics that gives Na and K a better capability for optimizing the CBO. However, both Na and K possess larger ionic sizes than Cu, leading to increased interfacial energies to 0.138 J/m^2 for Na and 0.151 J/m^2 for K. Such small changes are far from detrimental, as discussed above.

Indeed, the dramatic benefit of K to CBO is consistent with recent experiment, in which sequential post-deposition treatment with NaF and KF results in better performance.[6] However, K possesses much larger ionic size, and might introduce structural instability. This can be estimated by considering a simple decomposition energy (ΔE), defined as

$$\Delta E = E(A_2Se) + \frac{3}{2}[E(Cu\,In\,Se_2) + E(Cu\,In_5\,Se_8)] - E(A_2Cu_3\,In_9\,Se_{16}),$$

where A is an alkali element. For Na, $\Delta E = 4.7$ kcal/mol, implies spontaneous formation of doped structure. For K, on the other hand, $\Delta E = -16.7$ kcal/mol shows a relatively strong tendency of the doped structure to decompose. Therefore, we suggest that the performance can be optimized by tuning the ratio of Na to K to be optimal, with K improving the CBO and Na stabilizing the doping.

The remaining interface model, $CdCu_3In_9Se_{16}$/CdS, shown in Figure 4(c), uncovers the effects of intermixing at the interface. The CBO is compliantly tuned by the increase in the band gap, very likely due to the Cu vacancy, while the Cd impurity does not seem to play a significant role. Similarly, the interfacial energy increases further to 0.225 J/m^2, which again is not a substantial effect.

IV. CONCLUSION

To elucidate the effects of defects on band offsets at CIGS/CdS interfaces, we applied the B3PW91 hybrid functional and used average electrostatic potentials for reference levels to obtain the offsets. We first validated our methodology with benchmark calculations on pristine $CuInSe_2$/CdS interfaces for both nonpolar (110) and polar (112) cases. We found that an interface-interface distance of around 10 Å, is sufficient for good convergence of interface geometry, interfacial energy, and band offsets. We validated that these results (VBO = 0.73 eV) lead to excellent agreement with experiment, VBO = 0.8 ± 0.1 eV.

We also evaluated the core level method for predicting band offsets, but we found both poor convergence and poor

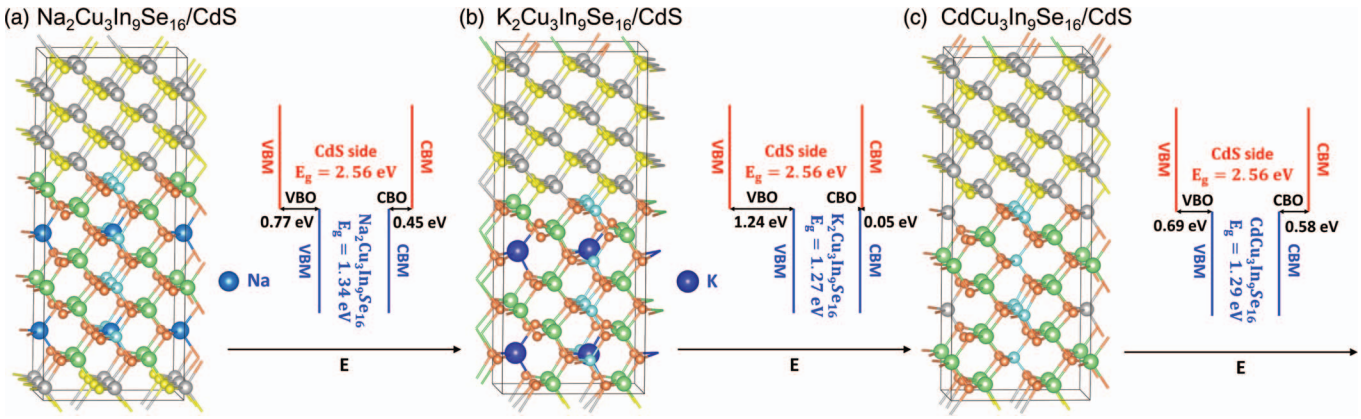

FIG. 4. The interface models and calculated band alignments of (a) $Na_2Cu_3In_9Se_{16}$/CdS, which increases the band bap by 0.27 eV while decreasing the CBO by 0.38 eV, (b) $K_2Cu_3In_9Se_{16}$/CdS, which increases the band bap by 0.20 eV while decreasing the CBO by 0.78 eV, and (c) $CdCu_3In_9Se_{16}$/CdS, which increases the band bap by 0.22 eV while decreasing the CBO by 0.35 eV.

accuracy, suggesting that core levels provide poor reference levels for predicting band offsets with hybrid functionals.

Our studies show that band offsets depend only weakly on the surface orientation (increasing by 0.04 eV for the polar (112) vs nonpolar (220)), which is consistent with experimental observations.

We then built optimized models of bulk CIGS structures having various defect or dopant compositions and carried out calculations for the interface to CdS. Here we investigate the effects on both band offsets and interfacial energies.

We find that band gap widening (by 0.13 eV) by Ga alloying (with Cu-rich phases) results only in modifying the VBO, with the CBO staying near 0.83 eV, far too large for an efficient solar cell.

However, we find that introducing at the interface Cu vacancy concentrations close to experiment leads to a dramatic decrease in the CBO to 0.46 eV, a nearly satisfactory value (best performance is expect for <0.4 eV). We find that the Cu vacancies eliminate the dominance of the Cu 3*d* levels on the VBM. This removes the sensitivity of the VBM to band gap engineering, enabling tunability of the CBO. This shows that Cu vacancies play a critical importance on performance.

Furthermore, we show that addition of alkali elements Na and K improves the CBO, but via a different mechanism. Here they elevate the VBM and thus CBM (band gap region) through electrostatics. The effect of Na is to decrease CBO slightly to 0.45 eV, which may explain the improved performance with Na. We predict that K has a much stronger effect on CBO than Na, reducing CBO to 0.05 eV. However, we find that K tends to destabilize the defect phase, whereas Na stabilizes it. Thus we propose that the performance of CIGS devices may be further optimized through tuning the ratio of Na to K.

On the other hand, Cd dopants lead to a slight increase in CBO to 0.58 eV, indicating possible deleterious effects.

Finally, all defects and dopants tend to decrease the interfacial stability, but the magnitude seems small enough (0.01–0.18 J/m^2) to be only a minor issue.

ACKNOWLEDGMENTS

We are grateful to Dr. Jamil Tahir-Kheli and Dr. Ravishankar Sundararaman for helpful discussions. This work was initiated with support from Dow Solar and completed with support from by the Joint Center for Artificial Photosynthesis (JCAP), a DOE Energy Innovation Hub, supported through the Office of Science of the U.S. Department of Energy under Award No. DE-SC0004993.

[1]REN21, *Renewables 2013 Global Status Report* (REN21 Secretariat, Paris, 2013).
[2]A. Jäger-Waldau, *PV Status Report 2013* (Publications Office of the European Union, Luxembourg, 2013).
[3]K. L. Chopra, P. D. Paulson, and V. Dutta, Prog. Photovoltaics **12**, 69 (2004).
[4]P. Jackson, D. Hariskos, E. Lotter, S. Paetel, R. Wuerz, R. Menner, W. Wischmann, and M. Powalla, Prog. Photovoltaics **19**, 894 (2011).
[5]A. Chirilă, S. Buecheler, F. Pianezzi, P. Bloesch, C. Gretener, A. R. Uhl, C. Fella, L. Kranz, J. Perrenoud, S. Seyrling, R. Verma, S. Nishiwaki, Y. E. Romanyuk, G. Bilger, and A. N. Tiwari, Nat. Mater. **10**, 857 (2011).
[6]A. Chirilă, P. Reinhard, F. Pianezzi, P. Bloesch, A. R. Uhl, C. Fella, L. Kranz, D. Keller, C. Gretener, H. Hagendorfer, D. Jaeger, R. Erni, S. Nishiwaki, S. Buecheler, and A. N. Tiwari, Nat. Mater. **12**, 1107 (2013).
[7]D. Schmid, M. Ruckh, F. Grunwald, and H. W. Schock, J. Appl. Phys. **73**, 2902 (1993).
[8]D. Schmid, M. Ruckh, and H. W. Schock, Appl. Surf. Sci. **103**, 409 (1996).
[9] U. Rau and H. W. Schock, Appl. Phys. A **69**, 131 (1999).
[10]M. Kemell, M. Ritala, and M. Leskelä, Crit. Rev. Solid State Mater. Sci. **30**, 1 (2005).
[11]R. Klenk, Thin Solid Films **387**, 135 (2001).
[12]J. Hedstrom, H. Ohlsen, M. Bodegard, A. Kylner, L. Stolt, D. Hariskos, M. Ruckh, and H. Schock, in *Photovoltaic Specialists Conference, 1993, Conference Record of the Twenty Third IEEE, Louisville, KY, 10–14 May* (IEEE, 1993), pp. 364–371.
[13]K. Granath, M. Bodegård, and L. Stolt, Sol. Energy Mater. Sol. Cells **60**, 279 (2000).
[14]D. Rudmann, Ph.D. thesis, Swiss Federal Institute of Technology (ETH), Zürich, 2004.
[15]A. Rockett, Thin Solid Films **480–481**, 2 (2005).
[16]S. Ishizuka, A. Yamada, M. M. Islam, H. Shibata, P. Fons, T. Sakurai, K. Akimoto, and S. Niki, J. Appl. Phys. **106**, 034908 (2009).
[17]F. Couzinié-Devy, N. Barreau, and J. Kessler, Prog. Photovoltaics **19**, 527 (2011).
[18]D. J. Schroeder and A. A. Rockett, J. Appl. Phys. **82**, 4982 (1997).
[19]L. E. Oikkonen, M. G. Ganchenkova, A. P. Seitsonen, and R. M. Nieminen, J. Appl. Phys. **114**, 083503 (2013).
[20]T. Nakada and A. Kunioka, Appl. Phys. Lett. **74**, 2444 (1999).
[21]D. Liao and A. Rockett, J. Appl. Phys. **93**, 9380 (2003).
[22]O. Cojocaru-Mirédin, P. Choi, R. Wuerz, and D. Raabe, Appl. Phys. Lett. **98**, 103504 (2011).
[23]C.-S. Jiang, F. S. Hasoon, H. R. Moutinho, H. A. Al-Thani, M. J. Romero, and M. M. Al-Jassim, Appl. Phys. Lett. **82**, 127 (2003).
[24]E. S. Mungan, W. Xufeng, and M. A. Alam, IEEE J. Photovoltaic **3**, 451 (2013).
[25]P. Hohenberg and W. Kohn, Phys. Rev. **136**, B864 (1964).
[26]W. Kohn and L. J. Sham, Phys. Rev. **140**, A1133 (1965).
[27]S. B. Zhang, S. H. Wei, and A. Zunger, Phys. Rev. Lett. **78**, 4059 (1997).
[28]C. H. Chang, S.-H. Wei, J. W. Johnson, S. B. Zhang, N. Leyarovska, G. Bunker, and T. J. Anderson, Phys. Rev. B **68**, 054108 (2003).
[29]C. D. R. Ludwig, T. Gruhn, C. Felser, and J. Windeln, Phys. Rev. B **83**, 174112 (2011).
[30]S.-H. Wei, S. B. Zhang, and A. Zunger, J. Appl. Phys. **85**, 7214 (1999).
[31]J. Kiss, T. Gruhn, G. Roma, and C. Felser, J. Phys. Chem. C **117**, 10892 (2013).
[32]J. Kiss, T. Gruhn, G. Roma, and C. Felser, J. Phys. Chem. C **117**, 25933 (2013).
[33]S. Lany and A. Zunger, Phys. Rev. Lett. **93**, 156404 (2004).
[34]S. Lany and A. Zunger, Phys. Rev. Lett. **100**, 016401 (2008).
[35]L. E. Oikkonen, M. G. Ganchenkova, A. P. Seitsonen, and R. M. Nieminen, J. Phys.: Condens. Matter **23**, 422202 (2011).
[36]J. P. Perdew and M. Levy, Phys. Rev. Lett. **51**, 1884 (1983).
[37]L. J. Sham and M. Schluter, Phys. Rev. Lett. **51**, 1888 (1983).
[38]I. A. Vladimir, F. Aryasetiawan, and A. I. Lichtenstein, J. Phys.: Condens. Matter **9**, 767 (1997).
[39]F. Aryasetiawan and O. Gunnarsson, Rep. Prog. Phys. **61**, 237 (1998).
[40]A. D. Becke, J. Chem. Phys. **98**, 5648 (1993).
[41]J. K. Perry, J. Tahir-Kheli, and W. A. Goddard, Phys. Rev. B **63**, 144510 (2001).
[42]J. K. Perry, J. Tahir-Kheli, and W. A. Goddard, Phys. Rev. B **65**, 144501 (2002).
[43]J. Muscat, A. Wander, and N. M. Harrison, Chem. Phys. Lett. **342**, 397 (2001).
[44]J. Heyd, J. E. Peralta, G. E. Scuseria, and R. L. Martin, J. Chem. Phys. **123**, 174101 (2005).
[45]H. Xiao, J. Tahir-Kheli, and W. A. Goddard, J. Phys. Chem. Lett. **2**, 212 (2011).
[46]R. Dovesi, V. R. Saunders, C. Roetti, R. Orlando, C. M. Zicovich-Wilson, F. Pascale, B. Civalleri, K. Doll, N. M. Harrison, I. J. Bush, P. D'Arco, and M. Llunell, *CRYSTAL 2009 User's Manual* (University of Torino, Torino, 2009).
[47]R. Dovesi, C. Roetti, C. Freyria-Fava, M. Prencipe, and V. R. Saunders, Chem. Phys. **156**, 11 (1991).
[48]A. Lichanot, E. Aprà, and R. Dovesi, Phys. Status Solidi B **177**, 157 (1993).

[49]L. R. Kahn and W. A. Goddard, J. Chem. Phys. **56**, 2685 (1972).
[50]C. F. Melius and W. A. Goddard, Phys. Rev. A **10**, 1528 (1974).
[51]W. J. Stevens, M. Krauss, H. Basch, and P. G. Jasien, Can. J. Chem. **70**, 612 (1992).
[52]See supplementary material at http://dx.doi.org/10.1063/1.4893985 for optimized basis sets, density of states of Cu-rich and Cu-poor phases, energies and structures for model bulks with defects, coordinates and symmetry constraints of all inter-face models.
[53]J. E. Peralta, J. Heyd, G. E. Scuseria, and R. L. Martin, Phys. Rev. B **74**, 073101 (2006).
[54]H. J. Monkhorst and J. D. Pack, Phys. Rev. B **13**, 5188 (1976).
[55]C. G. Van de Walle and R. M. Martin, Phys. Rev. B **35**, 8154 (1987).
[56] G. Paasch and E. von Faber, Prog. Surf. Sci. **35**, 19 (1990).
[57]V. R. Saunders, C. Freyria-Fava, R. Dovesi, L. Salasco, and C. Roetti, Mol. Phys. **77**, 629 (1992).
[58]V. R. Saunders, C. Freyria-Fava, R. Dovesi, and C. Roetti, Comput. Phys. Commun. **84**, 156 (1994).
[59]T. Löher, W. Jaegermann, and C. Pettenkofer, J. Appl. Phys. **77**, 731 (1995).
[60]S. H. Wei and A. Zunger, Appl. Phys. Lett. **63**, 2549 (1993).
[61]T. Schlenker, V. Laptev, H. W. Schock, and J. H. Werner, Thin Solid Films **480–481**, 29 (2005).
[62]T. Schulmeyer, R. Hunger, A. Klein, W. Jaegermann, and S. Niki, Appl. Phys. Lett. **84**, 3067 (2004).
[63]T. Minemoto, T. Matsui, H. Takakura, Y. Hamakawa, T. Negami, Y. Hashimoto, T. Uenoyama, and M. Kitagawa, Sol. Energy Mater. Sol. Cells **67**, 83 (2001).
[64]S. Levcenko, N. N. Syrbu, E. Arushanov, V. Tezlevan, R. Fernández-Ruiz, J. M. Merino, and M. León, J. Appl. Phys. **99**, 073513 (2006).
[65]E. Cadel, N. Barreau, J. Kessler, and P. Pareige, Acta Mater. **58**, 2634 (2010).